

Article

A Novel Remaining Useful Life Prediction Approach for Superbuck Converter Circuits Based on Modified Grey Wolf Optimizer-Support Vector Regression

Li Wang ^{1,*}, Jiguang Yue ¹, Yongqing Su ¹, Feng Lu ² and Qiang Sun ¹

¹ College of Electronic and Information Engineering, Tongji University, No. 4800, Cao'an Highway, Shanghai 201804, China; yuejiguang@tongji.edu.cn (J.Y.); yongqingsu@163.com (Y.S.); qiangsun@outlook.com (Q.S.)

² School of Ocean and Earth Science, Tongji University, No. 1239, Siping Road, Shanghai 200092, China; LF@tongji.asia

* Correspondence: 2015wangli@tongji.edu.cn; Tel.: +86-021-6958-9241

Academic Editors: Laura Ramirez Elizondo and Frede Blaabjerg

Received: 9 January 2017; Accepted: 20 March 2017; Published: 2 April 2017

Abstract: The reliability of power packs is very important for the performance of electronic equipment and ensuring the reliability of power electronic circuits is especially vital for equipment security. An alteration in the converter component parameter can lead to the decline of the power supply quality. In order to effectively prevent failure and estimate the remaining useful life (RUL) of superbuck converters, a circuit failure prognostics framework is proposed in this paper. We employ the average value and ripple value of circuit output voltage as a feature set to calculate the Mahalanobis distance (MD) in order to reflect the health status of the circuit. Time varying MD sets form the circuit state time series. According to the working condition time series that have been obtained, we can predict the later situation with support vector regression (SVR). SVR has been improved by a modified grey wolf optimizer (MGWO) algorithm before estimating the RUL. This is the first attempt to apply the modified version of the grey wolf optimizer (GWO) to circuit prognostics and system health management (PHM). Subsequently, benchmark functions have been used to validate the performance of the MGWO. Finally, the simulation results of comparative experiments demonstrate that MGWO-SVR can predict the RUL of circuits with smaller error and higher prediction precision.

Keywords: superbuck converter circuit; prognostics and system health management (PHM); remaining useful life (RUL) prediction; support vector regression (SVR); modified grey wolf optimizer (MGWO)

1. Introduction

Energy shortage makes the power supply system attract considerable attention, and the study of converter circuits in this system has become a focus. As the core part of a switching power supply, the converter circuit is mainly responsible for voltage conversion, power transmission and other functions. Its function determines its important position in energy conversion. It is worth mentioning that the superbuck converter circuit is the research object of this study (the superbuck converter is widely used in aerospace power systems because it can bring high efficiency to the solar power system). Even if the circuit topology changed, the data-driven fault prediction method will still be feasible. In this study, the superbuck converter circuit is employed as an example to introduce the remaining useful life (RUL) Prediction Approach.

Due to the fact the converter is directly connected with all kinds of electronic equipment, the reliability and safety of the converter circuit are the premise to guarantee that the other electronic

equipment can work normally. When the converter is running, all circuit components are slowly degrading. The degradation of the components will have a variety of effects on the circuit, which may even lead to circuit failure. The parametric fault is a kind of soft fault, which will cause the circuit performance and output characteristics to gradually change and will eventually cause system structural failure. Therefore, the prediction of parametric faults is very important for the realization of circuit RUL prediction.

The failure prediction of power electronics circuits is of great significance for complex industrial applications including the energy industry, aerospace, automotive, and space applications. However, converter circuit test is still a crucial and challenging task in the domain of circuit prognostics and system health management (PHM) due to the difficulties involving consideration of component tolerances, complex fault mechanisms, and the effects of the operational and environmental stresses, etc. Unexpected circuit failures can lead to a series of problems such as performance degradation, function loss and even catastrophic failure, and hence, prevention of circuit failures is necessary and very desirable.

In order to achieve a technical breakthrough, a new method containing fault diagnosis and failure prognostics is proposed in response to the proper time and conditions, which is PHM. PHM is one of the most promising disciplines with potential technologies and methods in order to address reliability and the problem of maintainability of systems [1].

PHM is defined as “a maintenance and asset management approach utilizing signals, measurements, models, and algorithms to detect, assess, and track degraded health, and to predict failure progression” [2]. The main functionalities of PHM contain two concepts, namely fault diagnosis and failure prognostics. Therefore, both fault diagnosis and failure prognostics are necessary in order to complete circuit PHM.

The objective of circuit fault diagnosis is to assess the current state of the circuit and identify the faulty components, and the goal of circuit failure prognostics is to accurately estimate the remaining useful life (RUL) of the circuit. The prevention of circuit failures during field operation requires methods for the following: (1) the early detection and isolation of faults and (2) the prediction of the remaining useful performance (RUP) of the failing circuit [3]. Therefore, state of health (SOH) assessment and RUL estimation are among the key issues in PHM for circuit, and have been an active area of research for many years. By observing and evaluating the circuit SOH, impending failures can be predicted. After learning the key information about RUL, one can take the necessary precautions [4].

Generally, RUL prediction includes two main approaches: model-based methods and data-driven methods. As the structure of the circuit becomes more and more complex, the model is more and more difficult to build. The implementation of efficient and cost effective RUL prediction requirements is getting harder and harder. Due to the unavailability of fault models, converter circuit PHM is a challenging task. In order to overcome the difficulties, people have tried various schemes, in which the data-driven method is relatively the most effective and convenient method. The reason that data-driven techniques stand out in many ways is because they do not require knowledge of the material properties, structure, or failure mechanisms. Data-driven methods are only dependent on the state of the circuit test data. Therefore, our work employs the method of failure prognostics based on a data-driven strategy.

At present, the main difficulties in the research of converter circuit RUL prediction are as follows: the failure modes of the circuit and the components are difficult to establish, as are the method of extracting the characteristic parameters of the circuit, and developing the matching prediction algorithm. Thanks to the rapid development of machine learning and other methods, data-driven methods are some of the current RUL prediction mainstream research methods. We can find many works for prognostics based on data-driven approaches [5–8]. Taking into account the significance of RUL prediction, we reckon it is necessary to continue in-depth research in this area.

At present, there is some representative literature in this aspect: Ye et al. [9] proposed a methodology for health condition assessment of power supplies based on a database containing

degradation characteristics. Zhou and Du et al. [10,11] chose the output capacitor of the target circuit as the target component and recorded the voltage waveform data. Capacitance value is the function parameter of the capacitor. The component will not complete the stored energy and filtering function, when the capacitance value drops to a certain value. Then, the system will lose stability, and the circuit can be judged to be in failure mode. Then by processing these data with certain algorithms, they plotted the time variation curves for the reliability prognostic model. Wu et al. [12–17] analysed the failure mechanism and failure mode of key components and decided the failure thresholds of the parameters. Then, they proposed a failure prediction method for DC-DC converters. There is a lot of similar literature, but these articles do not focus on the prediction algorithm, that is, in-depth study of the selection of parameters. Zhou and Feng [18,19] used a deterioration injection method to verify the equivalent series resistance (ESR) greater impact on DC-DC converter from the angle of physics experiments. Wang [20] proposed a method of online residual life prediction based on a nonlinear degradation model. Chen [21] proposed a power MOSFET degradation modeling and lifetime prognosis overall research program. Chen [22] studied the failure mechanism and failure model of key components of power circuits such as capacitor, power MOSFET, power diode and the characteristic failure parameters which can reflect the failure mode of the components. Jia's research [23] focused on the prediction algorithm, he proposed GA-GM and PSO-NGM fault prediction models for buck-boost converter circuit based on the gray system GM(1, 1) model. However, the prediction accuracy needs to be further improved. Li et al. [24] proposed a particle filter (PF) approach to RUP prediction. Hu et al. [25] also adopt a PF approach to model adaption and RUL prediction. However, it is very difficult for us to establish the PF state observation equation, and the initial process of the PF is complex. Hence, these methods are not very practical in actual converter circuit situations. Considering the maturity of support vector regression (SVR) theory and the high prediction accuracy, we use SVR method to RUL prediction. For SVR, the selection of key parameters has a great influence on the prediction results. In the literature, PSO is often used as an optimization tool for the purpose of training SVR parameters. However, grey wolf optimizer (GWO), regardless of the speed or the optimization effect is better than PSO. After some improvements to the inherent shortcomings of the GWO method, we apply it to SVR parameter optimization. Therefore, our study provides an alternative solution to converter circuit RUL prediction with better solutions.

This paper is structured as follows: Section 2 describes the circuit RUL prediction implementation routine. Section 3 introduces the necessary circuit principle of the superbuck converter. Section 4 shows how to deal with the extracted feature set by Mahalanobis distance (MD), and then construct the degradation curve of circuit health status. Section 5 gives the foundation of SVR. Section 6 studies the parameter estimation of SVR based on modified grey wolf optimizer (MGWO). Section 7 discusses RUL prediction implement results and discussions. Finally, Section 8 is devoted to conclusions.

2. Implementation Routine

Due to fact it is a fourth-order system for which it is difficult to obtain an accurate model, it is challenging to develop PHM methods for superbuck converter circuits. Data-driven approaches are more suitable for superbuck converter circuit RUL prediction because they do not rely on the prior knowledge, such as the topology of the circuit, the material properties of the components, and the degradation failure mechanism of the circuit, so a data-driven method is adopted to predict the RUL of a superbuck converter circuit in this context.

When the converter is running, the circuit components are slowly degrading. The best way to monitor the health status of the circuit is to monitor all its components. However, the degradation of components is very difficult to monitor. It is easy on the other hand to monitor and measure the output of the circuit. Therefore, we collect the output voltage, which is used to get the feature set to reflect the status of the converter circuit.

An overview of the proposed prognostic framework for the circuit under test (CUT) is shown in Figure 1. In our work, first the output voltage of CUT is collected. The mean value and the ripple of

the output voltage are selected to establish the feature set. Then, the feature set can be used to calculate a fault indicator (FI) whose value can reflect the performance of the circuit. The failure threshold is defined by the value of FI when the component reaches the failure boundary (namely, fails). Then, MGWO is utilized to adjust the parameter of SVR. Finally, RUL prediction based on MGWO-SVR is used to predict the model. When the value of FI reaches the failure threshold, the RUL of the circuit would be estimated.

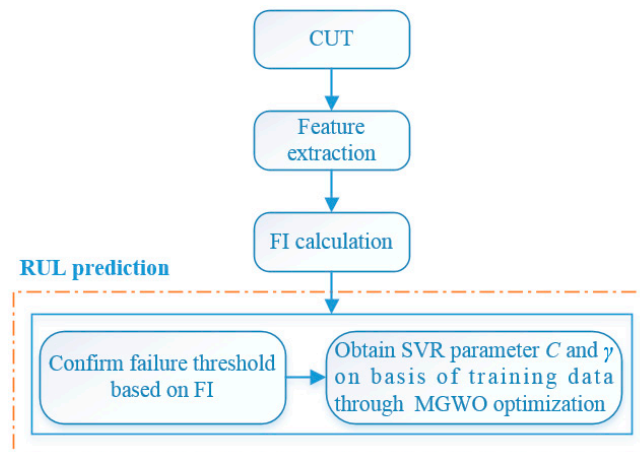


Figure 1. Overview of remaining useful life (RUL) prediction framework for circuit under test (CUT).

3. Circuit Principle of Superbuck Converter

The discussion assumes that the superbuck converter is operating in continuous conduction mode (CCM). Besides, the duty cycle of PWM is a fixed value. The superbuck converter is a fourth-order system which made up of two inductors and two capacitors. The superbuck converter circuit topology is shown in Figure 2.

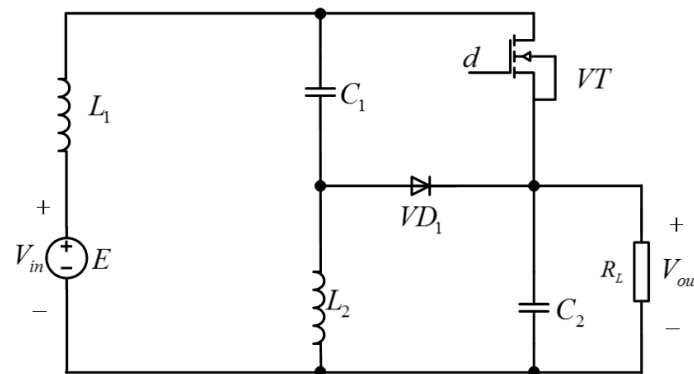


Figure 2. Superbuck converter circuit topology.

When the switch VT is turned on, the diode VD_1 will shut off. The power supply E provides the energy to the capacitor C_2 and the load resistance R_L through the inductance L_1 and switch VT , and the inductance L_2 passes through the capacitance C_1 and switch VT to provide the energy to the capacitor C_2 and the load resistance R_L . Therefore, the current through the switch VT is equal to the sum of the current through the inductance L_1 and inductance L_2 . When the switch VT is turned off, the diode VD_1 is in a state of conduction. Power E is supplies through the inductor L_1 to charge the capacitor C_1 , while the power supply E and inductance L_2 through the diode VD_1 to provide the energy to the capacitor C_2 and the load resistance R_L . Therefore, the current through the diode VD_1 is also equal to the sum of current through the inductance L_1 and inductance L_2 .

We find that the mean value and the ripple of the output voltage are very sensitive to any changes of the parameters of the components in the circuit, so the two physical quantities are used to measure the health status of the circuit. We take two components as an example. If the load resistance R_L varies with time, the change of the output voltage curve is shown in Figure 3; If the capacitor C_2 varies with time, the change of the output voltage curve is shown in Figure 4.

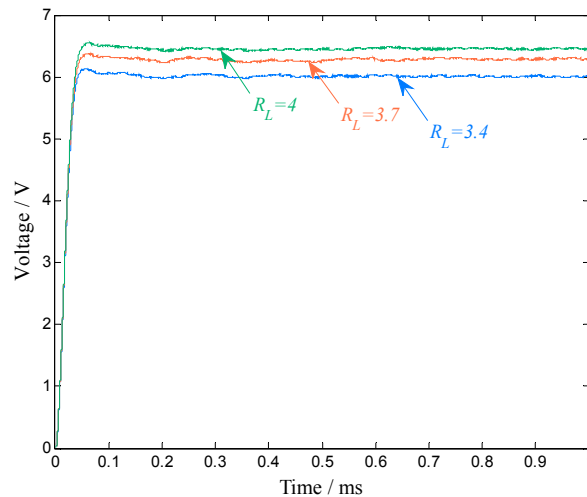


Figure 3. Output voltage curves with respect to different value of R_L .

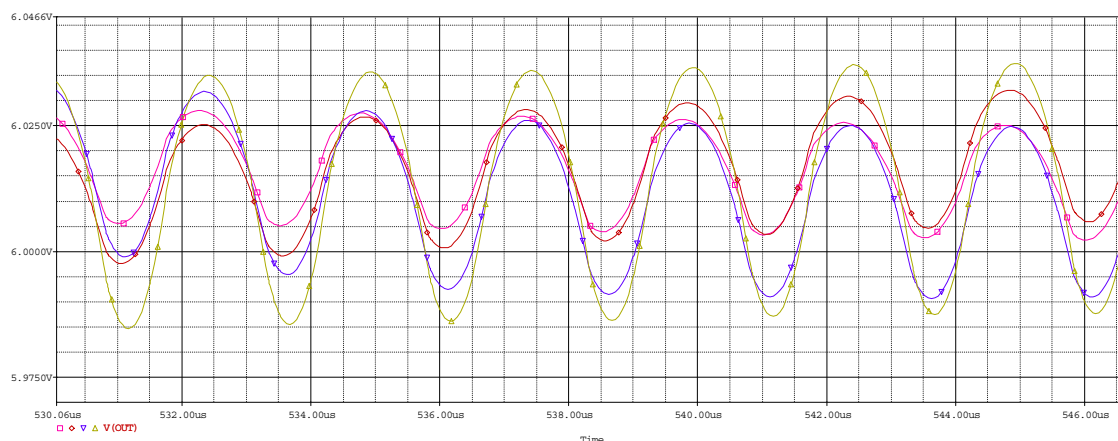


Figure 4. Output voltage curves with respect to different value of C_2 (Steady state).

The change of the component value can obviously affect the mean value and the ripple of the output voltage, so it can be used to monitor the degradation of the circuit by tracking the mean value and the ripple of the output voltage. Therefore, the mean value and the ripple of the output voltage are selected to establish the feature set.

4. Degradation Curve of Circuit Health Status Constructed by Extracted Feature Set

In our attempt at predict RUL, we try to extract meaningful information from the original data. In order to accomplish this, we need to know something about feature extraction. The extracted features are an important basis for the characterization of the degree of circuit health status. In our work, we can collect the feature set of the circuit as the parameter values change.

The mean value and the ripple of the output voltage are extracted as the feature vector $[\bar{V}, \Delta V]$ when the output voltage is stable. All feature vectors of the circuit with the changes of the parameter

values can be collected to form a feature set. The feature set will be processed to reflect the health status of CUT, and MD is selected to address this task and further complete the establishment of the FI.

MD can indicate the correlation between the two vectors, but also can be understood as the degree of deviation between each other. Assuming that $\mathbf{X}(n \times p)$ is a data matrix. The MD between the i -th row vector $\mathbf{X}_i = (x_1, x_2, \dots, x_p)_i$ of \mathbf{X} and the mean vector $\bar{\mathbf{X}}(1 \times p)$ of \mathbf{X} is calculated as follows:

$$MD_i = \sqrt{(\mathbf{X}_i - \bar{\mathbf{X}})\mathbf{C}_X^{-1}(\mathbf{X}_i - \bar{\mathbf{X}})^T} \quad (1)$$

where \mathbf{C}_X is variance covariance matrix; $i = 1, 2, \dots, n$.

Assuming that \mathbf{X}_i means the characteristics of the i -th health status; Assuming that \mathbf{X}_1 corresponds to the characteristic of the condition of no fault (normal state); as the component parameters deviate from the normal value gradually, \mathbf{X}_f just corresponds to the characteristic of the condition of fault; \mathbf{X}_f can also be understood as a threshold to distinguish between the fault state and the normal state. Assuming that $FI_i = 1 - MD_i$, then the variation of FI reflects the circuit failure degradation process.

Compared with other types of distance algorithm, MD does not need to preprocess the feature vector, which is very important if there is a high expectation for real time. When a component is fault free, the value of FI is equal to 1, and the value decreases with the increasing of the degree of degradation of the component value. With the example in Section 3, we construct the health status degradation curve with the change of the value of the load resistance R_L based on FI.

Assuming the load resistance R_L varies from 4Ω to 10Ω and its value raises 0.03Ω with each time index. The number of time indices is 200. Then, each time index refers to a FI value. Finally, we can obtain the health status degradation curve, which is shown in Figure 5. From Figure 5, we can see the trend of degradation when the load resistance R_L changes its value. It denotes that feature extraction method is appropriate for representing the circuit failure trends.

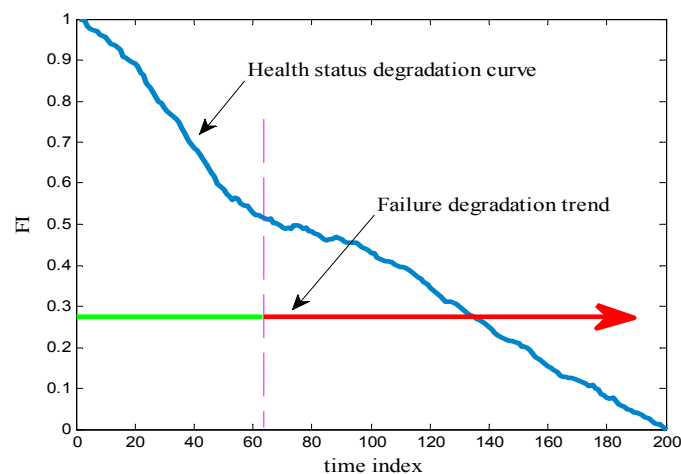


Figure 5. Health status degradation curve of load resistance R_L .

5. Support Vector Regression

5.1. SVR Theoretical Background

Methods for establishing the failure modes, extracting the characteristic parameters and drawing degradation curve of the circuit are described above. The following will introduce how to build a matching prediction algorithm.

SVM was proposed by Vapnik et al. [26] in the 1990s based on the theory of structural risk minimization (SRM), which came from statistical learning theory [27]. SVR is an application of SVM to the regression problem, and it has been widely used in many fields [28–31]. The principle of an SVR model can be briefly described as follows:

Assuming that a set of training set is given as $\mathbf{S} = \{(x_i, y_i), i = 1, 2, \dots, l\}$, where x_i is the i -th element of input vector in l -dimensional space, y_i is the actual value corresponding to x_i . The linchpin of SVR is to seek the fitting function $f(x) = \mathbf{w}^T \boldsymbol{\varphi}(x) + b$ to make it best fit the training set \mathbf{S} that has been given. In order to acquire the model of degradation failure in this paper, we should obtain the regression model $f(x)$ which can be achieved by learning a sample set \mathbf{S} . A non-linear mapping $\boldsymbol{\varphi}(x)$ is defined to map the input data (training data) x_i into the so-called high dimensional feature space. Then, in the high dimensional feature space, there theoretically exists a linear function f , to formulate the non-linear relationship between input data and output data. Such a linear function, namely SVR function, is often written as Equation (2):

$$f(x) = \mathbf{w}^T \boldsymbol{\varphi}(x) + b \quad (2)$$

where $f(x)$ denotes the forecasting values. $\boldsymbol{\varphi}(x)$ is the mapping function of kernel space for extracting the character from the original space. The \mathbf{w} is a weight vector and b is the bias.

As mentioned above, the SVM method aims at minimizing the structure risk and reducing the complexity of the model. The ε -insensitive loss function is defined as Equation (3):

$$err(y, f(x)) = \max(0, |y - f(x)| - \varepsilon) \quad (3)$$

Equation (2) can also be expressed as a form of Equation (4):

$$err(y, f(x)) = \begin{cases} 0, & |y - f(x)| \leq \varepsilon \\ |y - f(x)| - \varepsilon, & |y - f(x)| > \varepsilon \end{cases} \quad (4)$$

The SVR method purposes to find the optimum hyperplane and minimize the error between the training data and ε -insensitive loss function. The SVR minimizes the overall errors, mentioned above, as shown in Equation (5):

$$\min_{b, \mathbf{w}} \frac{1}{2} \mathbf{w}^T \mathbf{w} + C \sum_{i=1}^l \max(0, |y_i - \mathbf{w}^T \boldsymbol{\varphi}(x_i) - b| - \varepsilon) \quad (5)$$

After the introduction of the new variables $\tilde{\xi}_i, \check{\xi}_i$, Equation (5) can be rewritten as a form of Equation (6):

$$\min_{b, \mathbf{w}, \tilde{\xi}_i, \check{\xi}_i} \frac{1}{2} \mathbf{w}^T \mathbf{w} + C \sum_{i=1}^l (\tilde{\xi}_i + \check{\xi}_i) \quad (6)$$

with the constraints:

$$\begin{cases} -\varepsilon - \tilde{\xi}_i \leq y_i - \mathbf{w}^T \boldsymbol{\varphi}(x_i) - b \leq \varepsilon + \check{\xi}_i \\ \tilde{\xi}_i, \check{\xi}_i \geq 0 \end{cases}$$

By introducing the Lagrange multiplier $\check{\alpha}_i, \tilde{\alpha}_i, \check{\lambda}_i, \tilde{\lambda}_i \geq 0$, we can get Lagrange function of Equation (6) as shown in Equation (7):

$$\begin{aligned} & \min L(w, b, \tilde{\xi}_i, \check{\xi}_i, \check{\alpha}_i, \tilde{\alpha}_i, \check{\lambda}_i, \tilde{\lambda}_i) \\ & = \frac{1}{2} \mathbf{w}^T \mathbf{w} + C \sum_{i=1}^l (\tilde{\xi}_i + \check{\xi}_i) - \sum_{i=1}^l \check{\alpha}_i (\varepsilon + \tilde{\xi}_i + y_i - \mathbf{w}^T \boldsymbol{\varphi}(x_i) - b) \\ & \quad - \sum_{i=1}^l \tilde{\alpha}_i (\varepsilon + \check{\xi}_i - y_i + \mathbf{w}^T \boldsymbol{\varphi}(x_i) + b) - \sum_{i=1}^l (\check{\lambda}_i \tilde{\xi}_i + \tilde{\lambda}_i \check{\xi}_i) \end{aligned} \quad (7)$$

The solution of Equation (7) can be solved by its dual problem described as follows:

$$\begin{aligned} \max_{\widehat{\alpha}_i, \widetilde{\alpha}_i} & -\frac{1}{2} \sum_{i=1}^l \sum_{j=1}^l (\widehat{\alpha}_i - \widetilde{\alpha}_i) (\widehat{\alpha}_j - \widetilde{\alpha}_j) K(\mathbf{x}_i, \mathbf{x}_j) \\ & - \sum_{i=1}^l \varepsilon (\widehat{\alpha}_i + \widetilde{\alpha}_i) + \sum_{i=1}^l y_i (\widehat{\alpha}_i - \widetilde{\alpha}_i) \end{aligned} \quad (8)$$

with the constraints:

$$\begin{cases} \sum_{i=1}^l (\widehat{\alpha}_i - \widetilde{\alpha}_i) = 0 \\ 0 \leq \widehat{\alpha}_i, \widetilde{\alpha}_i \leq C \end{cases}$$

where $K(\mathbf{x}_i, \mathbf{x}_j) = \boldsymbol{\varphi}(\mathbf{x}_i)^T \boldsymbol{\varphi}(\mathbf{x}_j)$. For non-linear regression problems, we can transform them into linear regression problems with the help of kernel function. Finally, the SVR function is obtained as Equation (9) successfully:

$$f(x) = \sum_{i=1}^l (\widehat{\alpha}_i - \widetilde{\alpha}_i) K(\mathbf{x}_i, \mathbf{x}) + b \quad (9)$$

where $b = y_i - \sum_{i=1}^l (\widehat{\alpha}_i - \widetilde{\alpha}_i) K(\mathbf{x}_i, \mathbf{x}) + \varepsilon$.

5.2. Kernel Functions

Common examples of kernel functions defined on Euclidean space \mathbb{R}^d include:

Linear kernel:

$$K(\mathbf{x}, \mathbf{y}) = \mathbf{x}^T \mathbf{y}, \mathbf{x}, \mathbf{y} \in \mathbb{R}^d$$

Polynomial kernel:

$$K(\mathbf{x}, \mathbf{y}) = (\gamma \mathbf{x}^T \mathbf{y} + r)^p, \mathbf{x}, \mathbf{y} \in \mathbb{R}^d, \gamma, r > 0$$

Gaussian kernel (RBF Kernel):

$$K(\mathbf{x}, \mathbf{y}) = \exp(-\gamma \|\mathbf{x} - \mathbf{y}\|^2), \mathbf{x}, \mathbf{y} \in \mathbb{R}^d, \gamma > 0$$

Perceptron kernel:

$$K(\mathbf{x}, \mathbf{y}) = \tanh(\gamma \mathbf{x}^T \mathbf{y} + r), \mathbf{x}, \mathbf{y} \in \mathbb{R}^d, \gamma, r > 0$$

If there is no priori knowledge about the given data, the Gaussian kernel (RBF Kernel) is the best choice when the kernel function is needed. The SVM, adopt Gaussian kernel, may be able to obtain the estimate very smoothly, which explains why Gaussian kernel have an advantage of achieving good performance. Furthermore, the value provided by Gaussian kernel is inside the range (0, 1), which will make the calculation process becomes simple. Therefore, in this paper, we adopt Gaussian kernel when we perform SVR. According to the content mentioned above, the core problem is to how determine the parameter C and parameter γ , if we intend to obtain the best fitting function of the SVR model.

6. Parameter Estimation of SVR Based on MGWO

6.1. Grey Wolf Optimizer (GWO) Algorithm

The GWO is a powerful evolutionary algorithm developed recently. It was proposed by Mirjalili [32] in 2014. As a new heuristic optimization algorithm, it has the advantages of simplicity and efficiency. Relevant research results show that the new proposed algorithm is very efficient in solving the issue of non-convex optimization problems. This paper aims to adopt this novel swarm intelligence optimization algorithm to the prognostics and systems health management for electronic products.

6.1.1. Grey Wolf Behavior

The grey wolf (*Canis lupus*) belongs to Canidae animal family, at the top of the food chain, and it is regarded a top predator animal. Grey wolves are social animals. They are more likely to live in a pack. The average number of wolves in the pack is from 5 to 12. In their daily life, especially in the hunting process, they follow a very strict social hierarchy and task assignment pattern. This is one of their most particular features. The hierarchy structure of grey wolves is shown in Figure 6.

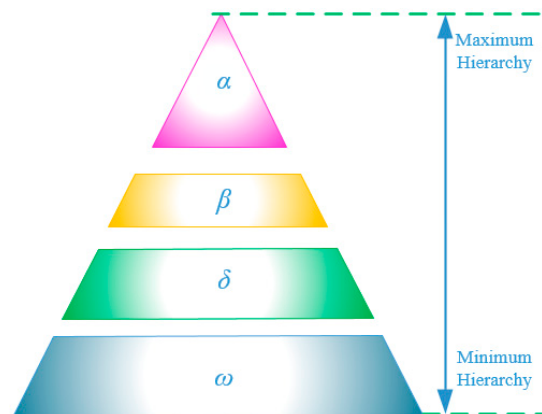


Figure 6. Hierarchy structure of grey wolves.

In the GWO algorithm, the highest level wolves are called the alpha wolves (α). The rest of the wolves according to social class are designated as beta wolves (β), delta wolves (δ) and omega wolves (ω). The alpha wolves which includes a male wolf and a female wolf are the head of the pack. As the leadership in the pack, they are responsible for the process of hunting (optimization) and decision-making about resting places, waking up time and other activities. On the other hand, some democratic behavior is also seen, in which alpha wolves obey the other wolves in the pack. While gathering, the whole team admits alpha wolves and obeys their commands. It is amazing and interesting that alpha wolves (α) are not necessarily the most powerful individuals but must be the best supervisors and managers. This indicates that compared to the power of alpha wolves (α) the organization and discipline of a pack is much more important.

The beta wolves (β) are in the third level up in the hierarchy structure of grey wolves shown in Figure 6. From the bottom up the number of the third layer are also the second level of the chain of command. The beta wolves (β) are the managers who help alpha wolves (α) monitor or lead the implementation of collective actions. The beta wolves (β) may also be female or male, and they will be the best successor if any of alpha wolves (α) dies or gets old. The beta wolves (β) should respect the alpha wolves (α), but the beta wolves (β) have the power right to order other wolves in the lower level in the hierarchy structure. They play a role of consultants for alpha wolves (α) and the trainers of the whole pack. They strengthen the influence of alpha wolves (α) in the entire pack, and give the pack feedback to the alpha wolves (α). The lowest ranking grey wolves are omega wolves (ω). The omega wolves (ω) can be the scapegoats for a couple of bad hunting results. The omega wolves (ω) are at the lowest level in the hierarchical structure of grey wolves, so they are subject to the other levels of wolves forever. They are finally allowed to eat after the prey is caught.

It seems that omega wolves (ω) have unimportant minor roles. However, when a situation such as the loss of the omega wolves (ω) occurs, the entire pack will face internal strife and a series of other issues. Therefore, the omega wolves (ω) are indispensable. Furthermore, the existence of omega wolves (ω) will make the configuration of the other whole team members more reasonable and perfect.

If a wolf is not an alpha wolf, beta wolf, or omega wolf, it is called a subordinate or delta wolf. The delta wolves (δ) must obey the alpha wolves (α) and the beta wolves (β), and also has the right to command the omega wolves (ω). Sentinels, scouts, elders, caregivers, and hunters belong to this

class. They are responsible for the observation of territory and territorial boundaries, and providing warnings in case of danger. The sentinels are in charge of protecting and ensuring the safety of the group. The scouts are responsible for monitoring the boundaries of the territory and warning when the group is in any danger. The elders are the most experienced wolves in the group and they are also powerful assistants of the alpha wolves (α) and the beta wolves (β). The caregivers are responsible for taking care of the weak, sick and injured wolves in the pack. Finally, the hunters help the alpha wolves (α) and the beta wolves (β) to find prey, and to provide the necessary food for the entire pack. In addition to the existence of a hierarchy structure among grey wolves, their group hunting is another interesting social behavior. According to the research findings published by Muro et al. [33], the main stages of group hunting are as follows:

- (1) Tracking, chasing and approaching the prey
- (2) Pursuing, surrounding and harassing the prey until it stops moving
- (3) Attacking the prey.

6.1.2. Mathematical Formulation of Social Behavior of Grey Wolves

In this section, we are about to describe the method of mathematically modelling the group behavior for wolves, and assume that alpha wolves (α) are the best solutions to the corresponding mathematical problem. The corresponding sub optimal solutions are considered as beta wolves (β), delta wolves (δ) and omega wolves (ω), respectively. The purpose of the design of the algorithm GWO is to find the fittest solution alpha wolves (α), and this algorithm take into account the group behavior of wolves including tracking, pursuing and attacking.

Encircling or Trapping Prey

To achieve the aforementioned goals, we use mathematical modeling method. At first, wolves surround the prey when hunting. We put forward the following equations to describe the process:

$$\vec{D} = \left| \vec{C} \cdot \vec{X}_{\text{Prey}}(t) - \vec{X}_{\text{GWolf}}(t) \right| \quad (10)$$

$$\vec{X}_{\text{GWolf}}(t+1) = \vec{X}_{\text{Prey}}(t) - \vec{A} \cdot \vec{D} \quad (11)$$

where t indicates the number of current iteration, \vec{A} and \vec{C} are coefficient vectors, \vec{X}_{Prey} is the position vector of prey to be hunted, \vec{X}_{GWolf} indicates the position vector of a grey wolf. \vec{A} provides random weights to search for prey in the search space. If the grey wolves diverge from each other position for chasing a prey, the random value \vec{C} can be forced to correct the deviation from the plan.

The coefficient vectors \vec{A} and \vec{C} can be calculated by the following equations:

$$\vec{A} = 2\vec{a} \cdot \vec{r}_1 - \vec{a} \quad (12)$$

$$\vec{C} = 2 \cdot \vec{r}_2 \quad (13)$$

where \vec{a} is linearly decreased from 2 to 0 with the increase of the number of iterations for better development and exploration of candidate solutions, and \vec{r}_1 and \vec{r}_2 are random vectors in $(0, 1)$.

Hunting of Prey

Grey wolves have the ability to identify the location of prey, and surround or capture them. The hunting activities of the packs are usually guided by the alpha wolves (α). The beta wolves (β), delta wolves (δ) are also involved in hunting prey. However, in a strange search space without a priori knowledge, in fact, we do not know the optimal solution (prey position). In order to mathematically

simulate the hunting behavior of the group, we assume that the alpha wolves (α) (the best candidate solution), the beta wolves (β) and the delta wolves (δ) have better potential for approaching the prey location. Therefore, we preserve the first three optimal solutions obtained so far and force the other members in the group to update their location according to the best three solutions. The following series of equations are rigorous mathematical description of the specification of this rule.

The scores and positions of the first three search agents (i.e., alpha wolves (α), beta wolves (β) and delta wolves (δ)) can be updated using Equations (6)–(8), respectively:

$$\vec{D}_{Alpha}(t) = \left| \vec{C}_1 \cdot \vec{X}_{Alpha}(t) - \vec{X}(t) \right| \quad (14)$$

$$\vec{D}_{Beta}(t) = \left| \vec{C}_2 \cdot \vec{X}_{Beta}(t) - \vec{X}(t) \right| \quad (15)$$

$$\vec{D}_{Delta}(t) = \left| \vec{C}_3 \cdot \vec{X}_{Delta}(t) - \vec{X}(t) \right| \quad (16)$$

The position vector of prey with respect to alpha wolves (α), beta wolves (β) and delta wolves (δ) can be calculated by the following mathematical equations:

$$\vec{X}_1(t) = \vec{X}_{Alpha}(t) - \vec{A}_1 \cdot \vec{D}_{Alpha}(t) \quad (17)$$

$$\vec{X}_2(t) = \vec{X}_{Beta}(t) - \vec{A}_2 \cdot \vec{D}_{Beta}(t) \quad (18)$$

$$\vec{X}_3(t) = \vec{X}_{Delta}(t) - \vec{A}_3 \cdot \vec{D}_{Delta}(t) \quad (19)$$

The best position can be obtained by the way calculating the average of the result of the Equations (17)–(19):

$$\vec{X}(t+1) = \frac{1}{3} \left(\vec{X}_1(t) + \vec{X}_2(t) + \vec{X}_3(t) \right) \quad (20)$$

6.2. Modified Grey Wolf Optimizer (MGWO) Algorithm

Although the GWO has the advantages of simplicity and high efficiency, we still feel that there is room for improvement in order to better adapt it to our application. In order to have a better global search capability and to avoid falling into a local optimum, we modified the original GWO algorithm.

We extend the search scope of GWO algorithm to the whole solution space in each iteration process, so as to construct a new algorithm MGWO. Its aim is to extend the search scope to the entire solution space in each iteration, so as to increase the probability of obtaining the global optimal solution, namely, to enhance the ability to obtain the optimal parameters of the SVR model. The specific update equations of MGWO is as follows:

$$\vec{X}_{1_update}(t) = \vec{X}_1(t) + \left[\vec{lb} + \left(\vec{ub} - \vec{lb} \right) \cdot \vec{r}_3 \right] \quad (21)$$

$$\vec{X}_{2_update}(t) = \vec{X}_2(t) + \left[\vec{lb} + \left(\vec{ub} - \vec{lb} \right) \cdot \vec{r}_4 \right] \quad (22)$$

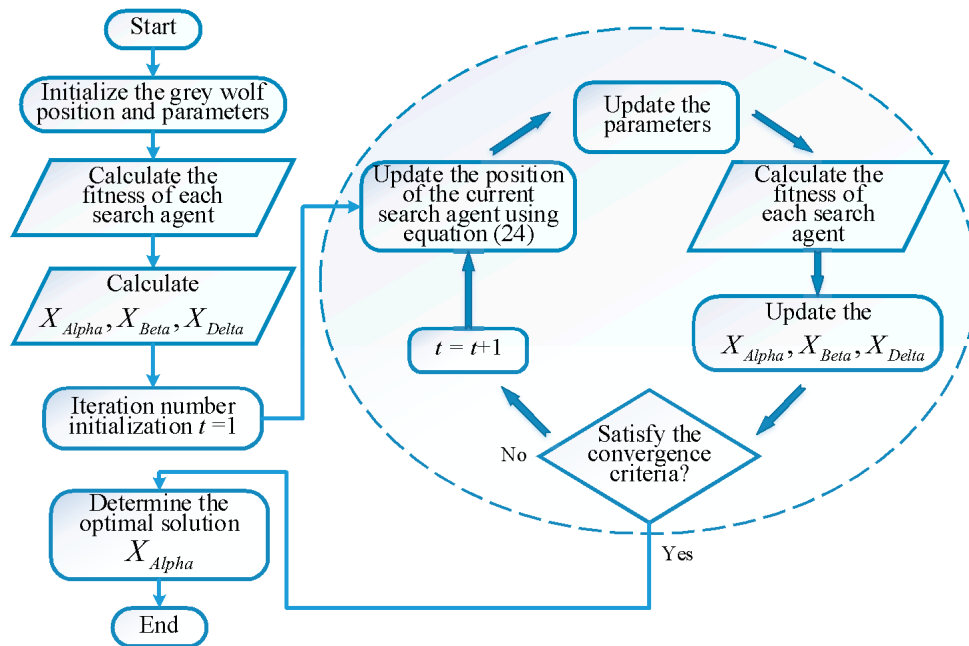
$$\vec{X}_{3_update}(t) = \vec{X}_3(t) + \left[\vec{lb} + \left(\vec{ub} - \vec{lb} \right) \cdot \vec{r}_5 \right] \quad (23)$$

Thus, the updated best position can be obtained by the way calculating the average of the result of the Equations (21)–(23):

$$\vec{X}_{update}(t+1) = \frac{1}{3} \left(\vec{X}_{1_update}(t) + \vec{X}_{2_update}(t) + \vec{X}_{3_update}(t) \right) \quad (24)$$

where $\vec{r}_3, \vec{r}_4, \vec{r}_5$ are random vectors in $(-1, 1)$, \vec{lb} and \vec{ub} are lower and upper bounds of group search space, respectively.

By expanding the search scope of the pack, the individual search scope is no longer confined to a specific range, which is conducive to the algorithm to jump out of the local optimal solution to obtain the global optimal solution. The flow-process diagram and pseudo code of MGWO is depicted in Figure 7a,b, respectively.



(a)

Pseudo code of the MGWO algorithm

```

Initialize the grey wolf population  $X_i, i = 1, 2, \dots, n$ 
Initialize  $a, A$  and  $C$ 
Calculate the fitness of each search agent

 $X_{Alpha}$  = the best search agent
 $X_{Beta}$  = the second best search agent
 $X_{Delta}$  = the third best search agent

While  $t < \text{Max number of iterations}$ 
  For each search agent
    Update the position of the current search agent using equation (24)
  End for
  Initialize  $a, A$  and  $C$ 
  Calculate the fitness of each search agent
  Update  $X_{Alpha}, X_{Beta}, X_{Delta}$ 
   $t = t + 1$ 
End while
Return  $X_{Alpha}$ 
  
```

(b)

Figure 7. The process (a) and pseudo code (b) of the modified grey wolf optimizer (MGWO).

6.3. Procedure of Parameter Estimation of SVR Using MGWO

In the prediction model, the parameter C and parameter γ are user-determined variables which play an important role in the performance of SVR using MGWO. MGWO algorithm has shown superior performance in parameter optimization. Hence, the algorithm is opted for estimating the parameter C and parameter γ for SVR in this work. The parameter C and parameter γ are corresponding to the position of each agent and the optimization target is to explore and dig out an optimal position. The flow-process diagram of the MGWO optimization is shown in Figure 7 and the detailed optimizing steps can be depicted as follows.

- (1) The penalty factor C and kernel function parameter γ of SVR are initialized, and the related parameters of MGWO algorithm are set up.
- (2) Randomly generate a wolf pack, where the position vector of each agent corresponds to the parameter C and parameter γ .
- (3) Calculate the fitness value of each agent, based on initial parameters C and γ , by the training set for learning. Fitness value function is the correct rate in the sense of k -fold cross-validation method.
- (4) According to the fitness value, the agents are divided into four grades.
- (5) Update the location of each agent according to the Equations (21)–(24).
- (6) Calculate the fitness value of each agent corresponds to the new location and compare it with the results of the previous iteration. If the fitness value is better than the previous fitness value, then the agent fitness value and position instead of the best of the original pack, otherwise keep the original results to continue the iteration.
- (7) If the number of iterations exceeds the maximum allowed number of times, the training is over, and the output of the group optimal location is the SVR optimal value, parameter C and parameter γ , otherwise jump to step 4.
- (8) The prediction model is established by using the optimal parameters parameter C and parameter γ , and the test set is used to predict the experimental results.

7. Experiments and Discussion

In this section, we will carry out an experimental validation of a super buck converter circuit failure prognostics framework. In order to fully test the performance of MGWO-SVR to prove its effectiveness and feasibility for RUL prediction, this section is divided into two parts. In the first part, we employ several representative benchmark functions to evaluate the performance of the optimization algorithm MGWO; In the second part, MGWO-SVR is applied to carry out the RUL prediction based on the degradation data of the critical components in the CUT. It is worthwhile to mention that the experimental data is obtained from the PSPICE circuit simulation software. The following experimental validation was implemented on a MATLAB 2013a Software environment which was run on an Intel Xeon(R) E5-2637 V2 @ 3.5 GHz CPU with 8 GB RAM.

7.1. Benchmark Function Test Experiment

7.1.1. Selection of Benchmark Functions

In order to conduct a performance evaluation of the proposed MGWO optimization algorithm, we need to select the appropriate benchmark functions for the experimental analysis. In order to be able to evaluate the performance of the algorithm from multiple perspectives, the choice of the test functions should be as far as possible with different structural characteristics. This study selects three representative standard test function to test the actual effect of the improved algorithm MGWO. Concrete expression of the benchmark functions is shown in Table 1, where n is the number of the elements in the variable x , i, j represent the ordinal value of elements, Dim is the number of the variables, $Range$ is the boundary of the function's search space, and f_{min} is the optimum.

Table 1. Benchmark functions.

Function Name	Dim	Range	f_{\min}
F1: $f_1(x) = \sum_{i=1}^n \left(\sum_{j=1}^i x_j \right)^2$	30	(−100, 100)	0
F2: $f_2(x) = \sum_{i=1}^n ix_i^4 + \text{random}(0, 1)$	30	(−1.28, 1.28)	0
F3: $f_3(x) = \sum_{i=1}^n [x_i^2 - 10 \cos(2\pi x_i) + 10]$	30	(−5.12, 5.12)	0

7.1.2. Comparative Experimental Results Analysis

The F1 function is a simple unimodal benchmark function. Therefore, almost all optimization algorithm can easily find the global optimal value of the function. Its simplicity is conducive to evaluate the performance of the convergence speed of the optimization algorithm. What's more, the variables in the function do not affect each other and gradient information is always pointing to the global optimum, and the global optimum is zero. 2-D versions of F1 and convergence curve of PSO, GWO, and MGWO are shown in Figure 8. From the graph, we can see that the surface of the function is relatively smooth, there are no additional extreme points. GWO and MGWO are better than PSO, not only in the convergence rate, but also in the accuracy of the fitness value. MGWO is also better than the original GWO. We can see that MGWO is close to the optimal value after about 430 iterations, however, the convergence value of GWO is less than approximately one order of magnitude in the same number of iterations.

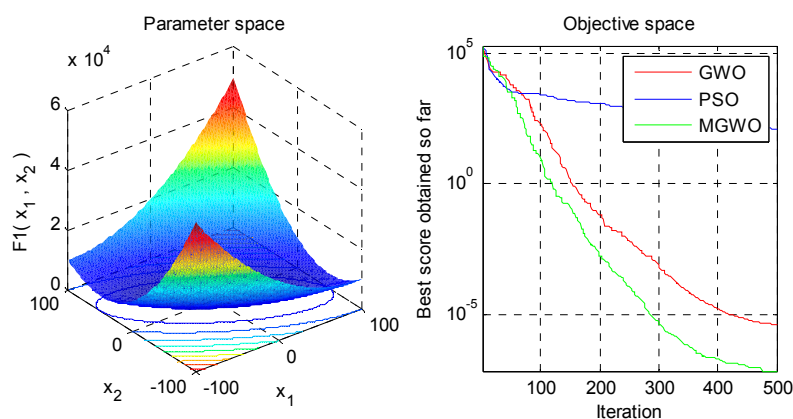


Figure 8. 2-D versions of F1 and convergence curve of particle swarm optimization (PSO), grey wolf optimizer (GWO), and MGWO.

The F2 function is also a unimodal benchmark function, but exists a large number of randomly arranged inflection point and deep local optima. Optimization algorithms very easily fall into a little extreme in the process of global optimization. The global optimum is 0. 2-D versions of F2 and convergence curve of PSO, GWO, and MGWO are shown in Figure 9. In the figure, we can see the GWO and MGWO iterative speed surpasses PSO. Then, due to the existence of a large number of local extreme points, the speed of MGWO and GWO, looking for the optimal value, are also slowed down in later iterations. It is worth mentioning that the performance of MGWO is still better than GWO.

The F3 function is a multimodal benchmark function, namely, it is a sphere with multiple peaks. There are also a large number of inflection points because of the cosine wave. The optimization algorithms in the process of the function of global optimization very easily fall into a local minimum point and cannot jump out of. The global optimum is also 0. 2-D versions of F3 and convergence curve of PSO, GWO, and MGWO are shown in Figure 10. Different from the F2 function, the F3 function is a multi-peak function, and the advantage of MGWO is obvious. In comparison, GWO and PSO are

no longer forward to the optimal solution after 150 iterations, because they fall into a local optimal solution. This result shows that MGWO has a great advantage in the face of multi-peak functions.

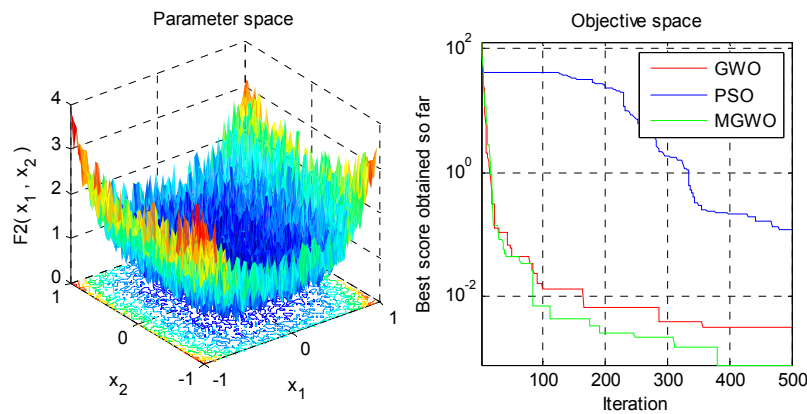


Figure 9. 2-D versions of F2 and convergence curve of PSO, GWO, and MGWO.

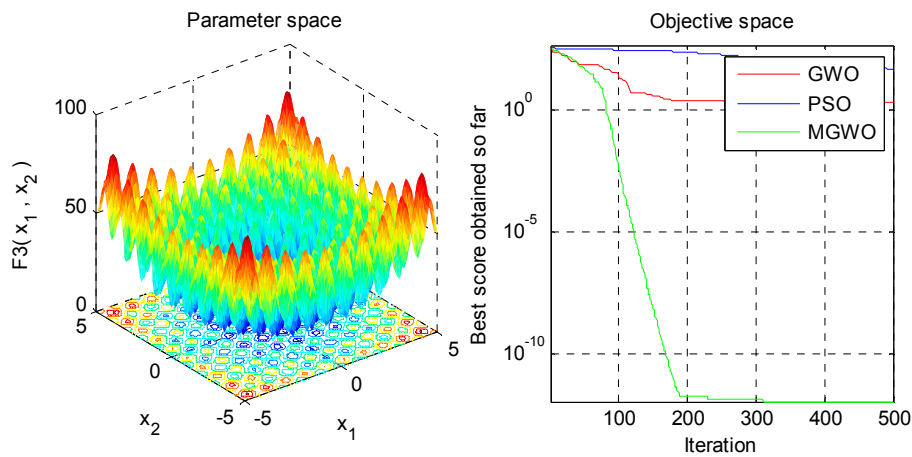


Figure 10. 2-D versions of F3 and convergence curve of PSO, GWO, and MGWO.

In order to make the experimental results more convincing, we have carried out the experiments 50 times for each function, and the corresponding results are recorded in Table 2.

Table 2. Results of benchmark functions.

Function Name	PSO		GWO		MGWO	
	Ave	Std	Ave	Std	Ave	Std
F1	77.2380	35.2769	3.46×10^{-5}	6.08×10^{-5}	2.41×10^{-6}	2.62×10^{-6}
F2	49.4660	5.9206	3.9850	2.9204	0.6772	1.3544
F3	0.1416	0.0407	0.00301	0.0010	0.0017	0.0005

Ave and std represent the mean and standard deviation of fitness values, respectively. According to the results of Table 2, MGWO is able to provide very competitive results. This algorithm outperforms all others in F1, F2, and F3. These results show the superior performance of MGWO in terms of exploiting the optimum. Namely, MGWO algorithm has merits in terms of exploration.

7.2. CUT Simulation Experiment

From the point of view of probability, single-fault conditions appear more frequently than multiple-fault conditions. Therefore, in this paper, a single-fault condition is selected to verify

the superbuck converter circuit failure prognostics framework based on MGWO-SVR. In order to fully explain the feasibility of the method, this paper carried out experiments on four key components as an example. The details of the CUT and the parameter settings are as described in the following subsections follows.

7.2.1. CUT Parameter Setting and Data Acquisition

Considering the influence of the parasitic parameters in the actual situation, we change the topology in Figure 2. The parasitic elements are added to the corresponding position, and the equivalent CUT diagram is shown in Figure 11. The topology of CUT is complex. It is worth mentioning that the switching period is equal to 2.5 μ s and the duty cycle is equal to 20%. The input voltage is equal to 20 V. The specific value of the other components is shown in Figure 11. Experimental analysis shows that many components have great influence on the output. In this paper, C_2 , L_1 , L_2 and R_L are selected as the object of RUL prediction.

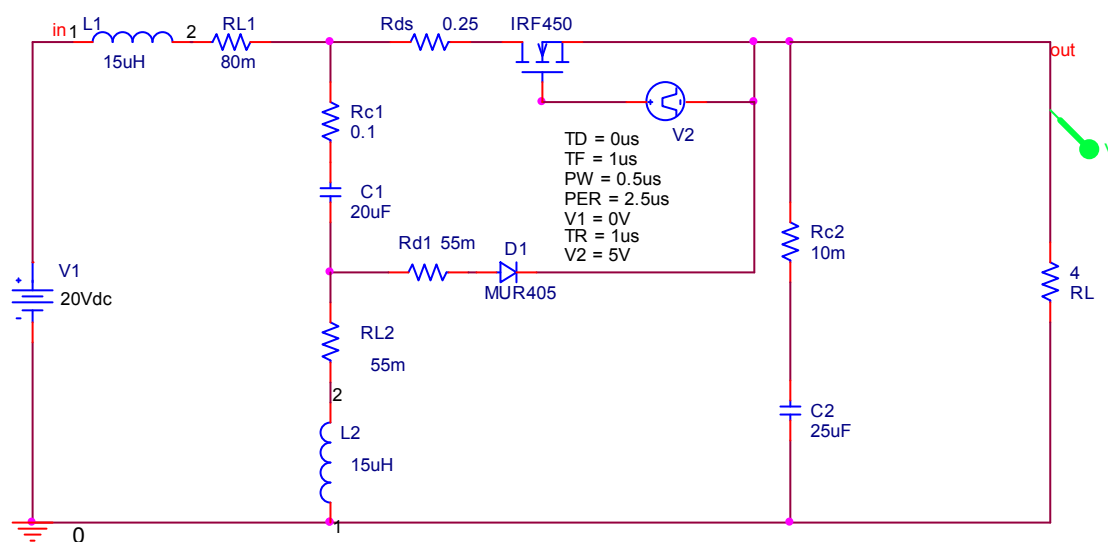


Figure 11. Superbuck converter circuit diagram constructed by PSPICE.

The circuit simulation experiment is carried out by the PSPICE software. PSPICE has established a common mathematical model of circuit components, and has a strong simulation ability. Therefore, PSPICE is a powerful software, and its simulation data has strong credibility. In this paper, the PSPICE parameters are set up to simulate the failure degradation process of the components. The response of the output side is used as a token of performance degradation, and it is used as the data of the subsequent prediction experiment. Specific experimental steps are described as follows:

We take R_L as an example to illustrate the RUL prediction approach proposed in Section 6. First of all, we need to establish the circuit schematic with the PSPICE software. The nominal value of R_L is 4 Ω . It is worth mentioning that, in the actual situation, to determine whether a circuit is faulty, we also need to consider the system stability and other issues. In this paper, we only consider the change of the parameter value. It is generally considered that a 50% deviation from the nominal value is considered a fault in academic circles [3]. Therefore, if the circuit component R_L is in the case of the failure that the parameter value of R_L is ascending, then the value of R_L deviates within the interval (4 ohm to 6 ohm). On the contrary, if the circuit component R_L is in the case of the failure where the parameter value of R_L is descending, then the value of R_L deviates within the interval (4 ohm to 2 ohm). In the paper, in order to simulate the change of the parameters to a greater extent, the values of the two kinds of cases are set to (4 ohm to 10 ohm) and (4 ohm to 1 ohm). In the case of increasing resistance value, we sample within the range of variation, and the difference between each value is the same. The total number of the sampling points is 200. Finally, we get a series of output response curves with the change of

the parameter value. The solution of FI can refer to Section 4. As is known, FI can reflect the degree of health of the CUT. Therefore, the FI curve is a useful tool for RUL prediction. We assume that the starting point (namely the data cutoff point for parameter estimation) for the RUL prediction when R_L deviates from its tolerance value at time index 40. Then, we use the data before time index 40 for MGWO-SVR parameter estimation. The PSPICE simulation parameters of the remaining components in the CUT to be tested can be set according to the R_L .

7.2.2. Results of CUT RUL Prediction

As is known from the last section, features are extracted by the PSPICE software and the FI is calculated through MATLAB. Component degradation is accompanied by a gradual change in the component value. After obtaining the degradation data of CUT, we should implement RUL prediction based on MGWO-SVR with MATLAB. Owing to space constraints and to get a better visual effect, the prediction data and the original data of FI are drawn together in the same picture.

Here, C_2 , L_1 , L_2 and R_L are selected as critical components. For critical component R_L , two types of degradation failure are considered: a class with fault value larger than the nominal value (labeled by \uparrow); the other with fault value smaller than the nominal value (labeled by \downarrow). Since the capacitance value and inductance value will only descend, we only consider this situation that fault value smaller than the nominal value (labeled by \downarrow) for C_2 , L_1 , L_2 . For the four example components in the CUT mentioned above, the following five different cases were studied. We implement comparative experiments of PSO-SVR, GWO-SVR and MGWO-SVR, and their RUL prediction results are shown in Figures 12–16.

- Case 1. Predict at time index 75 for $C_2\downarrow$.
- Case 2. Predict at time index 90 for $L_1\downarrow$.
- Case 3. Predict at time index 90 for $L_2\downarrow$.
- Case 4. Predict at time index 40 for $R_L\uparrow$.
- Case 5. Predict at time index 80 for $R_L\downarrow$.

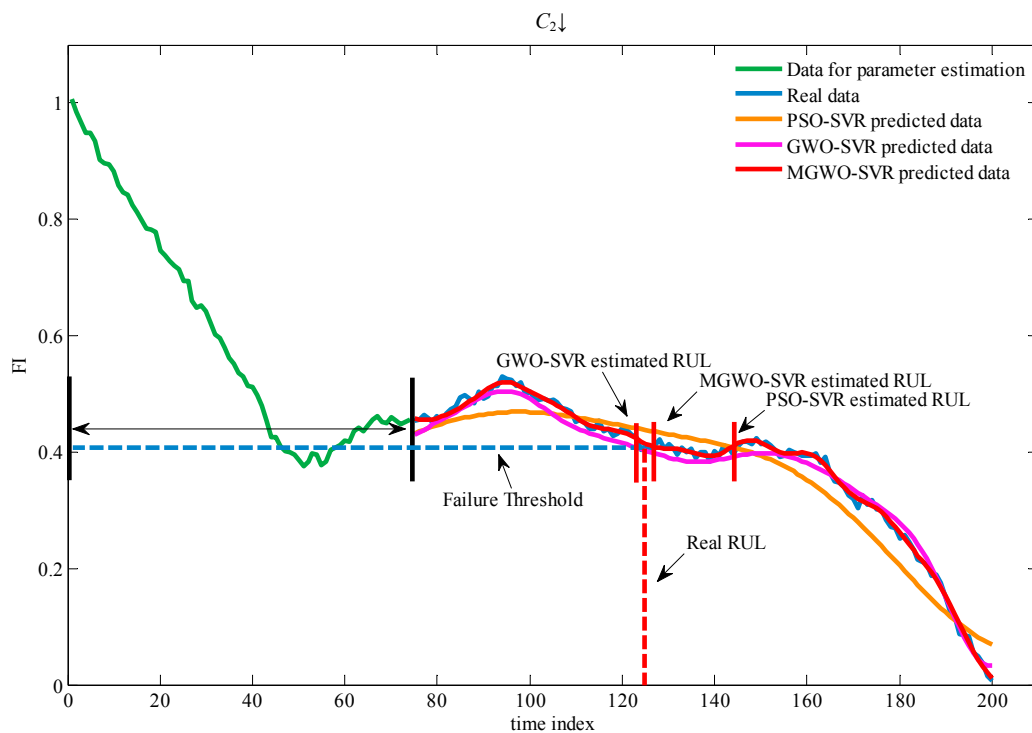


Figure 12. RUL prediction of Case 1.

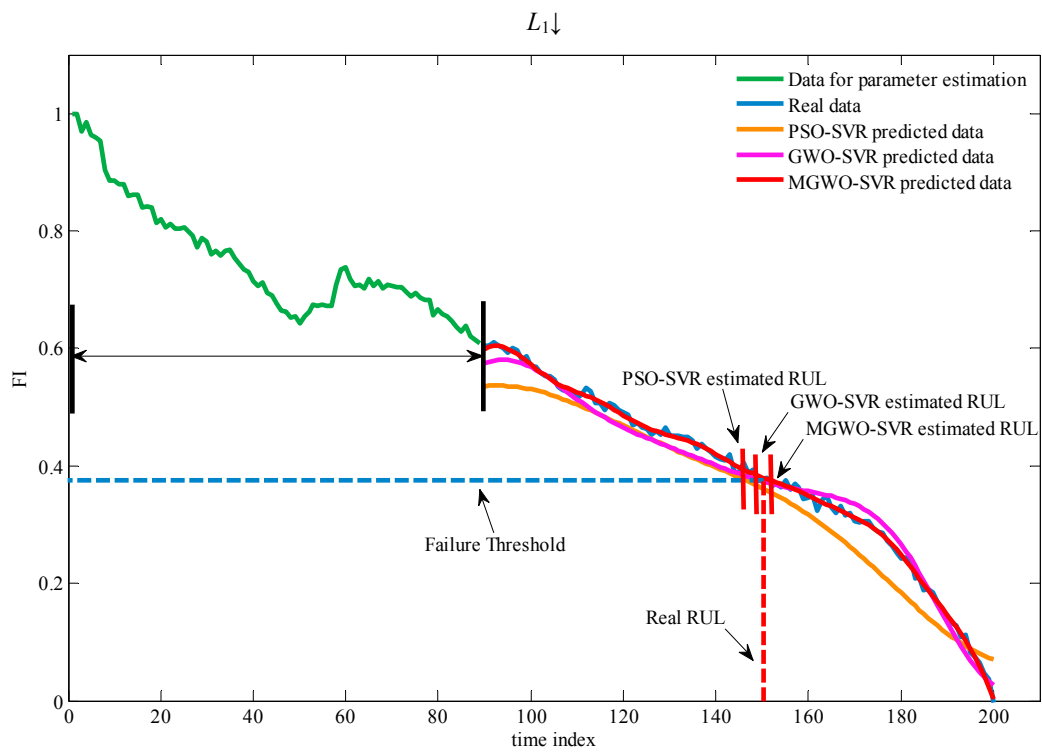


Figure 13. RUL prediction of Case 2.

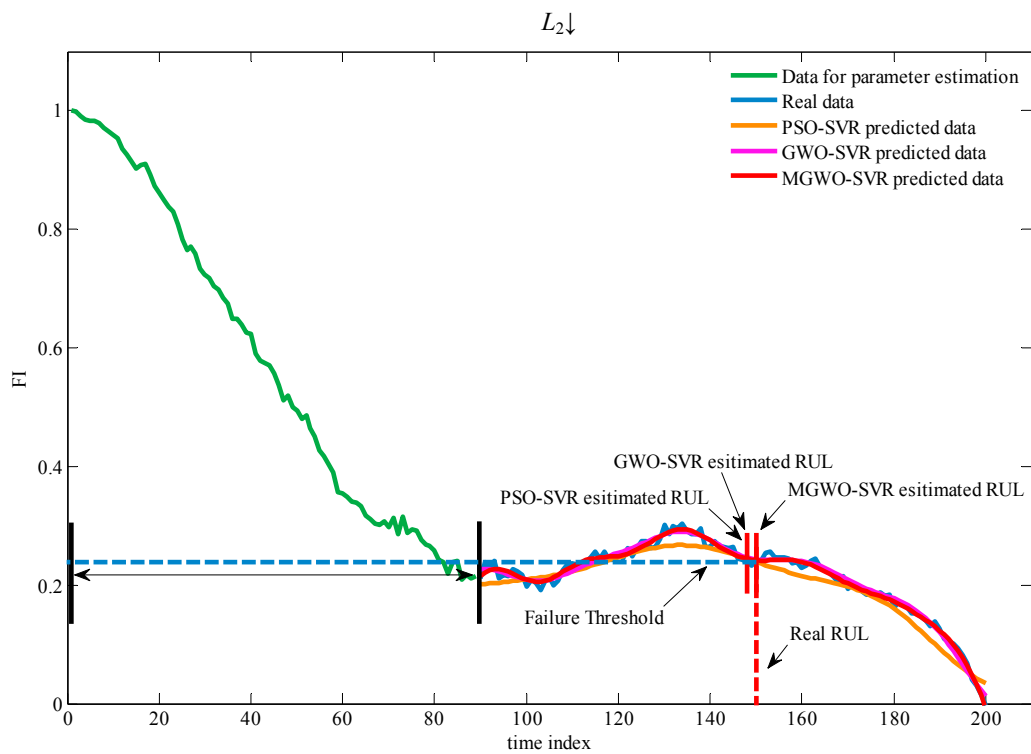


Figure 14. RUL prediction of Case 3.

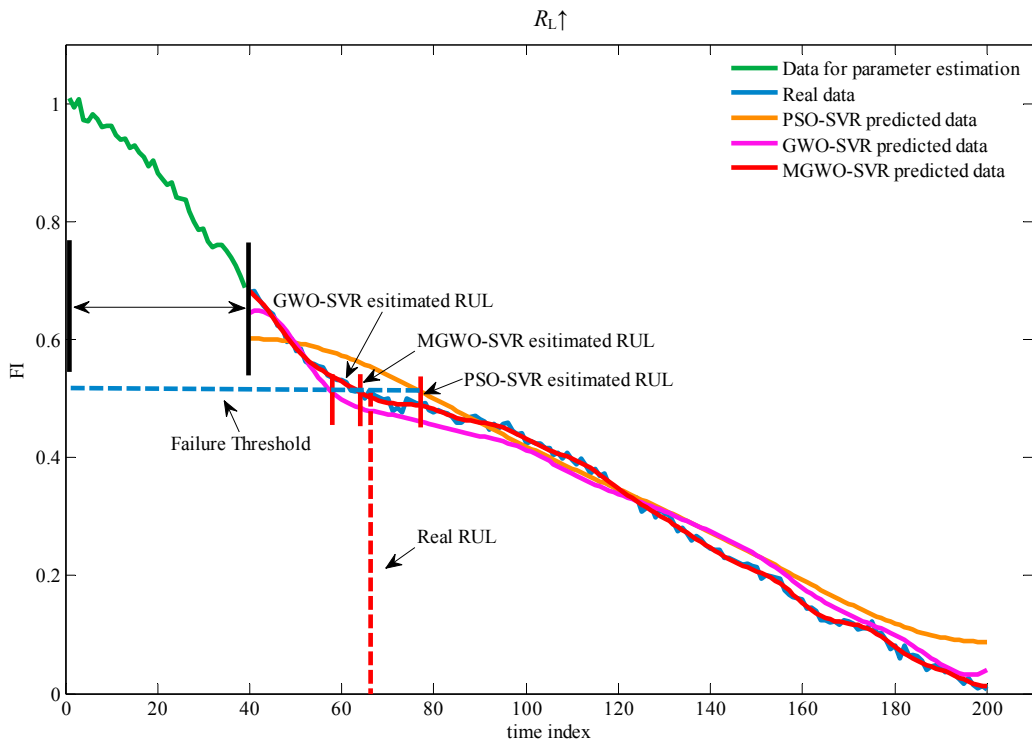


Figure 15. RUL prediction of Case 4.

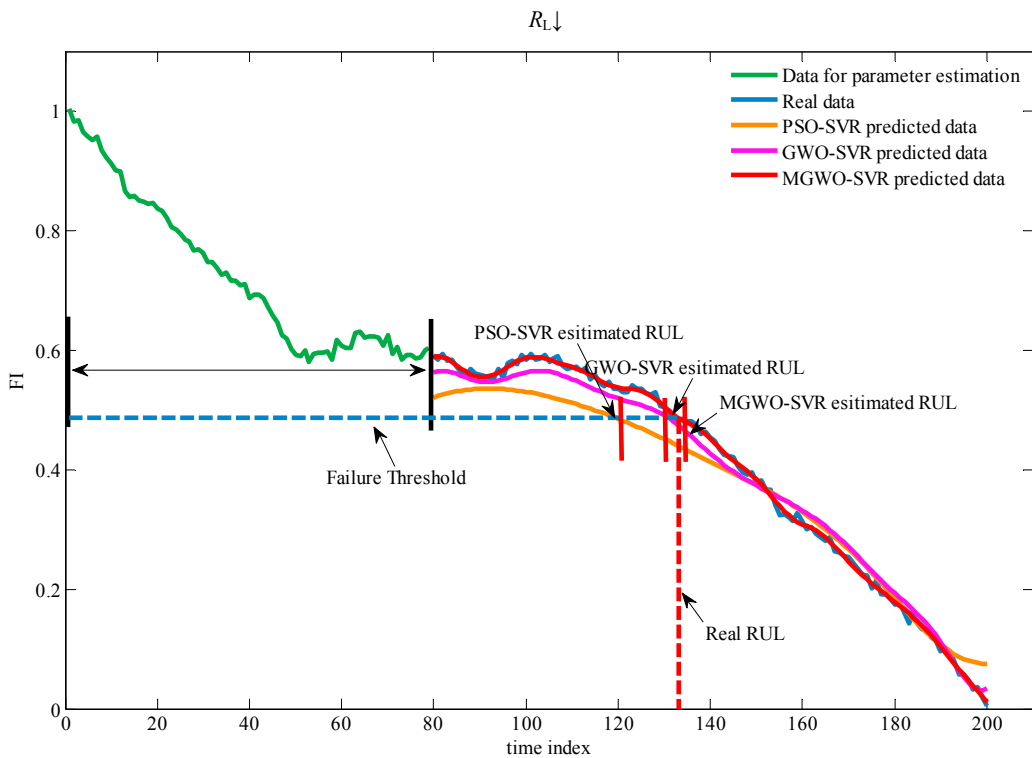


Figure 16. RUL prediction of Case 5.

For evaluating and analyzing the prediction performance from simulation experiment results in this paper, five commonly used error evaluation indicators, mean squared error (MSE), mean absolute

error (MAE), root mean squared error (RMSE), sum of squares for error (SSE) and Pearson correlation coefficient (PCC), as shown in Equations (25)–(29), are employed:

$$\text{MSE} = \frac{1}{N} \sqrt{\sum_{i=1}^N (x_i - y_i)^2} \quad (25)$$

$$\text{MAE} = \frac{1}{N} \sum_{i=1}^N |x_i - y_i| \quad (26)$$

$$\text{RMSE} = \sqrt{\frac{1}{N} \sum_{i=1}^N (x_i - y_i)^2} \quad (27)$$

$$\text{SSE} = \sum_{i=1}^N (x_i - y_i)^2 \quad (28)$$

$$\text{PCC} = \frac{\text{cov}(\mathbf{X}, \mathbf{Y})}{\sigma_X \sigma_Y} \quad (29)$$

Due to space limitations, we take Case 1 as an example to describe the RUL prediction result. The result for RUL prediction of CUT when component $C_2 \downarrow$ deviates from its nominal value to failure degradation are shown in Figure 12, represent the prediction result at time index 75. We set the failure threshold value according to the nominal value of 50%. That is, the failure threshold of $C_2 \downarrow$ is equal to FI when the value of C_2 is 12.5 nF (25 to $25 \times 50\%$). When the FI is lower than the failure threshold, the corresponding time index is determined to RUL. Real RUL and estimated RUL are corresponding to the first time index when FI is not greater than the failure threshold. Prediction error is the difference between real RUL and estimated RUL. MSE, MAE, RMSE, SSE and PCC are shown in Table 3, which can further measure the performance of MGWO-SVR. The actual RUL and predicted RUL of $C_2 \downarrow$ is 125 and 127 (carried out by MGWO), respectively. Therefore, 2 is the prediction error. It is equal to the result carried out by GWO. Except prediction error, the rest of the indicators carried out by MGWO are the best in Case 1. The results in Case 2–Case 5 show that MGWO has better solution than GWO and PSO, except for prediction error in Case 2. Based on the analysis of the results illustrated in Table 3, it can be clearly seen that proposed prognostic approach can predict the RUL of the critical components in CUT with small error. In other words, this approach can be effectively used for the aging degradation process RUL prediction of superbuck converter circuit.

Table 3. Results of Case 1–Case 5.

Cases	Case 1			Case 2			Case 3			Case 4			Case 5		
	PSO	GWO	MGWO												
Real RUL	125	125	125	150	150	150	150	150	150	66	66	66	133	133	133
Estimated RUL	144	123	127	146	149	152	149	149	150	77	58	64	121	131	134
Prediction error	19	2	2	4	1	2	1	1	0	11	12	2	12	2	1
MSE	0.1476	0.1291	0.0374	0.1627	0.1401	0.0291	0.0844	0.0711	0.0366	0.2007	0.1920	0.0406	0.2208	0.0990	0.0321
MAE	0.0231	0.0209	0.0052	0.0241	0.0235	0.0046	0.0131	0.0112	0.0054	0.0230	0.0265	0.0054	0.0332	0.0158	0.0049
RMSE	0.2087	0.1826	0.0529	0.2301	0.1982	0.0412	0.1193	0.1006	0.0517	0.2839	0.2715	0.0575	0.3123	0.1400	0.0454
SSE	0.0871	0.0667	0.0056	0.1059	0.0785	0.0034	0.0285	0.0202	0.0053	0.1612	0.1474	0.0066	0.1951	0.0392	0.0041
PCC	0.9772	0.9926	0.9985	0.9872	0.9917	0.9993	0.9778	0.9789	0.9938	0.9878	0.9875	0.9994	0.9942	0.9956	0.9995

8. Conclusions

RUL estimation has been an important engineering requirement for a long time. We aim at this goal and propose a MGWO-SVR-based prediction method to form a converter circuit fault prediction framework. In order to carry out experimental verification, we firstly collect the output voltage as feature set to calculate MD. Then, the FI which can represent the health state of the circuit can be obtained. The FI can be utilized to establish the failure degradation curve, which can be used to represent the health status trend. We select a part of the data before the initial prediction point for parameter estimation, and use the remaining data to test the RUL prediction performance. Detailed

simulation results of comparative experiments have demonstrated that MGWO-SVR has a strong ability for RUL prediction. The contributions of our work can be summarized as the following: We combine the theory with engineering practice. We improve the new heuristic optimization algorithm GWO, and employ it to adjust the SVR parameters. Then, a novel RUL prediction algorithm MGWO-SVR is proposed. This is its first application to superbuck converter circuit PHM, which is a hot but difficult field currently.

Acknowledgments: The authors would like to acknowledge the support of the State Administration of Science, Technology and Industry for National Defense (SASTIND) for their support of project's research and development in this area. This work comes from the special sub project MYHT funded by the Tongji University for SASTIND special research project "high reliability and long life span of Civil Aerospace products". Relevant agencies were also very helpful in providing feedback and support throughout the phase of this program.

Author Contributions: Li Wang and Jiguang Yue conceived and designed the experiment; Feng Lu, Li Wang and Yongqing Su analyzed the data. Li Wang and Qiang Sun wrote the manuscript.

Conflicts of Interest: The authors declare no conflict of interest.

References

1. Pecht, M.; Jaai, R. A prognostics and health management roadmap for information and electronics-rich systems. *Microelectron. Reliab.* **2010**, *50*, 317–323. [[CrossRef](#)]
2. Sheppard, J.W.; Kaufman, M.A.; Wilmering, T.J. IEEE standards for prognostics and health management. *IEEE Aerosp. Electron. Syst. Mag.* **2009**, *24*, 34–41. [[CrossRef](#)]
3. Vasan, A.S.S.; Long, B.; Pecht, M. Diagnostics and prognostics method for analog electronic circuits. *IEEE Trans. Ind. Electron.* **2013**, *60*, 5277–5291. [[CrossRef](#)]
4. Cui, Y.; Shi, J.; Wang, Z. Quantum assimilation-based state-of-health assessment and remaining useful life estimation for electronic systems. *IEEE Trans. Ind. Electron.* **2016**, *63*, 2379–2390. [[CrossRef](#)]
5. Alam, M.A.; Azarian, M.H.; Osterman, M.; Pecht, M. Prognostics of failures in embedded planar capacitors using model-based and data-driven approaches. *J. Intell. Mater. Syst. Struct.* **2011**, *22*, 1293–1304. [[CrossRef](#)]
6. Lee, C.M.; Ko, C.N. Short-term load forecasting using adaptive annealing learning algorithm based reinforcement neural network. *Energies* **2016**, *9*, 987. [[CrossRef](#)]
7. Han, L.; Narendran, N. An accelerated test method for predicting the useful life of an LED driver. *IEEE Trans. Power Electron.* **2011**, *26*, 2249–2257. [[CrossRef](#)]
8. Widodo, A.; Shim, M.C.; Caesarendra, W.; Yang, B.S. Intelligent prognostics for battery health monitoring based on sample entropy. *Expert Syst. Appl.* **2011**, *38*, 11763–11769. [[CrossRef](#)]
9. Ye, X.; Chen, C.; Wang, Y.; Zhai, G. Methodology research for health condition assessment of power supply based on simulation. *J. Syst. Simul.* **2015**, *27*, 185–191.
10. Zhou, H. Research on Reliability of Aluminum Electrolytic Capacitor in SMPS. Master's Thesis, Harbin Institute of Technology, Harbin, China, 2010.
11. Du, Y.; Guan, Y.; Wu, L.; Pan, W.; Wang, G.; Zhou, S. The impact of MOSFET and electrolytic capacitor on the DC-DC converter. *J. Digit. Content Technol. Appl.* **2011**, *3*, 170–180.
12. Wu, Y. Research on Fault Characteristic Parameters Extraction and Health Forecast Methods of Power Electronic Circuits. Master's Thesis, Nanjing University of Aeronautics and Astronautics, Nanjing, China, 2013.
13. Wu, Y.; Wang, Y.; Jiang, Y.; Lin, H. Fault prediction method of DC/DC converter based on characteristic parameter degradation. *Chin. J. Sci. Instrum.* **2013**, *34*, 181–188.
14. Jiang, Y.; Wang, Y.; Luo, H.; Lin, H.; Cui, J. An innovative metric for power electronic circuit failure evaluation and a novel prediction method based on LSSVM. *Trans. China Electrotech. Soc.* **2012**, *27*, 43–50.
15. Tan, X. Research of Failure Prediction of BUCK Circuit Based on Mahalanobis Distance. Master's Thesis, Nanjing University of Aeronautics and Astronautics, Nanjing, China, 2013.
16. Sun, F. Research on Fault Prediction Method of Power Electronic Circuit. Master's Thesis, Nanjing University of Aeronautics and Astronautics, Nanjing, China, 2010.
17. Wang, F. Study on Health Management for Intelligent Switching-Mode Power Supply. Master's Thesis, Chinese Academy of Sciences (Changchun Institute of Optics, Fine Mechanics and Physics), Changchun, China, 2015.

18. Zhou, S.; Guan, Y.; Wu, L.; Pan, W.; Wang, G.; Du, Y. Design and realization of DC-DC converter life prediction system based on LabView. *J. Conver. Inf. Technol.* **2011**, *6*, 300–308.
19. Feng, F. Research on Detection Method of Long Lifetime Aerospace DC/DC Converter. Master's Thesis, Xidian University, Xi'an, China, 2013.
20. Wang, S. Research on Online Reliability Estimation and Residual Life Prediction Method for On-Board Electronic Equipment. Master's Thesis, Nanjing University of Aeronautics and Astronautics, Nanjing, China, 2014.
21. Chen, S. Research on Degradation Model and Lifetime Prognosis Method for Power MOSFET. Master's Thesis, Harbin Institute of Technology, Harbin, China, 2013.
22. Chen, Y. Research on New Parameter Identification Methods and Failure Prediction Algorithms of Power Electronic Circuits. Master's Thesis, Nanjing University of Aeronautics and Astronautics, Nanjing, China, 2012.
23. Jia, Y. Research on Fault Prediction of the Power Electronic Devices Based on Improved Gray System. Master's Thesis, Nanjing University of Aeronautics and Astronautics, Nanjing, China, 2012.
24. Li, M.; Xian, W.; Long, B.; Wang, H. Prognostics of analog filters based on particle filters using frequency features. *J. Electron. Test.* **2013**, *29*, 567–584. [[CrossRef](#)]
25. Hu, Z.W.; Xiao, M.Q.; Zhang, L.; Song, H.F.; Yang, Z. Incipient fault diagnostics and remaining useful life prediction of analog filters. *J. Electron. Test.* **2015**, *31*, 461–477. [[CrossRef](#)]
26. Cortes, C.; Vapnik, V. Support-vector networks. *Mach. Learn.* **1995**, *20*, 273–297. [[CrossRef](#)]
27. Vapnik, V.N. An overview of statistical learning theory. *IEEE Trans. Neural Netw.* **1999**, *10*, 988–999. [[CrossRef](#)] [[PubMed](#)]
28. Chen, Y.H.; Hong, W.C.; Shen, W.; Huang, N.N. Electric load forecasting based on a least squares support vector machine with fuzzy time series and global harmony search algorithm. *Energies* **2016**, *9*, 70. [[CrossRef](#)]
29. Peng, L.L.; Fan, G.F.; Huang, M.L.; Hong, W.C. Hybridizing DEMD and quantum PSO with SVR in electric load forecasting. *Energies* **2016**, *9*, 221. [[CrossRef](#)]
30. Li, Z.X.; Rahman, S.M.M.; Vega, R.; Dong, B. A hierarchical approach using machine learning methods in solar photovoltaic energy production forecasting. *Energies* **2016**, *9*, 55. [[CrossRef](#)]
31. Zhang, Q.; Lai, K.K.; Niu, D.X.; Wang, Q.; Zhang, X.B. A fuzzy group forecasting model based on least squares support vector machine (LS-SVM) for short-term wind power. *Energies* **2012**, *5*, 3329–3346. [[CrossRef](#)]
32. Mirjalili, S.; Mirjalili, S.M.; Lewis, A. Grey wolf optimizer. *Adv. Eng. Softw.* **2014**, *69*, 46–61. [[CrossRef](#)]
33. Muro, C.; Escobedo, R.; Spector, L.; Coppinger, R.P. Wolf-pack (*Canis lupus*) hunting strategies emerge from simple rules in computational simulations. *Behav. Process.* **2011**, *88*, 192–197. [[CrossRef](#)] [[PubMed](#)]



© 2017 by the authors. Licensee MDPI, Basel, Switzerland. This article is an open access article distributed under the terms and conditions of the Creative Commons Attribution (CC BY) license (<http://creativecommons.org/licenses/by/4.0/>).